THE JOURNAL OF PHYSICAL CHEMISTRY B

Article

pubs.acs.org/JPCB

# Heat-Denatured Lysozyme Aggregation and Gelation As Revealed by Combined Dielectric Relaxation Spectroscopy and Light Scattering Measurements

A. Giugliarelli,[†] P. Sassi,[†] M. Paolantoni,[†] G. Onori,[‡] and C. Cametti*[,§]

[†]Department of Chemistry, University of Perugia, Via Elce di Sotto 8, I-06123 Perugia, Italy

[‡]Department of Physics, University of Perugia, Via A. Pascoli, I-06123 Perugia, Italy

[§]Department of Physics, University of Rome "La Sapienza" and CNR-INFM-SOFT, Piazzale A. Moro 5, I-00185 Rome, Italy

**ABSTRACT:** The dielectric behavior of native and heat-denatured lysozyme in ethanol–water solutions was examined in the frequency range from 1 MHz to 2 GHz, using frequency-domain dielectric relaxation spectroscopy. Because of the conformational changes on unfolding, dielectric methods provide information on the denaturation process of the protein and, at protein concentration high enough, on the subsequent aggregation and gelation. Moreover, the time evolution of the protein aggregation and gelation was monitored measuring, by means of dynamic light scattering methods, the diffusion coefficient of micro-sized polystyrene particles, deliberately added to the protein solution, which act as a probe of the viscosity of the microenvironment close to the particle surface. All together, our measurements indicate that heat-induced denaturation favors, at high concentrations, a protein aggregation process which evolves up to the full gelation of the system. These findings have a direct support from IR measurements of the absorbance of the amide I band that, because of the unfolding, indicate that proteins entangle each other, producing a network structure which evolves, in long time limit, in the gel.

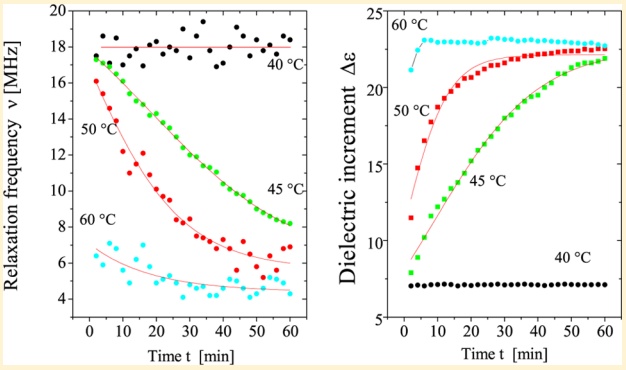


## 1. INTRODUCTION

It is well-known that alteration of the physicochemical properties of the suspending medium forces amphiphilic polymers to modify their structure, yielding, at high or relatively high concentrations, to the formation of extended networks with the consequence that the whole system gells.[1] The formation of heat-induced gels has been widely investigated in the past, in both their fundamental and applicative aspects.[2,3] However, the emerging scenario is rather intriguing since transparent solutions, turbid suspensions, transparent gels, and translucent and opaque gels have been observed, depending on physicochemical parameters, such as macromolecular concentration, pH, ionic strength, and temperature.[4]

Besides high-molecular-weight polymers, proteins and peptides as well are able to self-assemble into ordered supramolecular architectures on macroscopic or mesoscopic length scales. These protein structures have attracted considerable attention in the development of new biomaterials, thanks to their biocompatibility and biodegradability.[3,5,6]

The gelling process is favored by the unfolding of the polypeptide chains which leads to aggregation of denatured proteins.[7,8] During the heating process, the heat-induced denaturation causes proteins to lose their globular structures, exposing the hydrophobic residues to the surface. The presence of unfolded proteins and/or small aggregates at the first stage is important for the association of larger clusters and, further, for the formation of a gel.

In particular, lysozyme gelation can be induced by changes in the physicochemical properties of the solvent. The ability of lysozyme in aqueous–organic solvents to form optically transparent physical gels has been widely investigated over the past decade.[9−14] For example, binary mixtures such as tetramethylurea–water and dimethyl sulfoxide–water at room temperature induce physical gels consisting of transparent viscoelastic protein matrices.[15,16] The formation of transparent gels was also observed at high ethanol concentration, at room temperature.[17]

In a previous work,[18] some of us have investigated the aggregation behavior of (concentrated) lysozyme in ethanol–water solution by means of Fourier transform infrared absorption spectroscopy in the region of the amide I band. These measurements revealed that IR intensity at 1650 $cm^{-1}$ (indicative of the melting process) decreases as a function of temperature, whereas the intensity at 1618 $cm^{-1}$ (indicative of an aggregation precess) undergoes a pronounced increase, up

**Received:** June 16, 2012
**Revised:** July 16, 2012
**Published:** August 14, 2012

to the temperature at which the protein is in the unfolded conformation, followed by a marked decrease as the temperature is further increased.

Since this latter signal is assigned to the presence of intermolecular $\beta$-sheet conformation, its intensity increase has been interpreted as due to the formation of ordered aggregates which can evolve, in a defined temperature interval, toward the formation of a gel. At even higher temperatures, the further decrease of the intensity is attributed to the progressive destruction of the aggregates and to the tendency, for the single polypeptide chain, of acquiring again an unfolded conformation.

In this work, in order to observe the behavior of these systems at temperatures where gelation proceeds, we have investigated the aggregation and the gelling process of lysozyme in water−ethanol mixture solution at different temperatures, within the melting range, by means of two different techniques, i.e., dynamic light scattering and radiowave dielectric relaxation techniques.

Dielectric relaxation spectra give us information about charged structures that move under the influence of an applied electric field. In the frequency range of the experiment, i.e., in the megahertz frequency range, the observed relaxations are due to reorientational motion of protein aggregates and/or to fluctuation of free counterions between neighboring cross-linking points in the protein network.[19,20]

Here, dynamic light scattering techniques were employed to observe the translational diffusion of deliberately added monodisperse polystyrene latex particles in the protein solution in order to investigate the gel formation occurring at temperatures above denaturation. In this way, we are able to obtain information about the structure of the protein network by investigating the movement of particles of appropriate size incorporated in the gel network. Because of the progressive formation of the gel, the diffusion coefficient of the added particles reduces drastically, resulting a local probe of the changes taking place in the medium. The change in the viscosity properties during the gelation process is monitored by the use of the incorporated particle diffusion coefficient as a function of time.

Thanks to these complementary techniques, our results, all together, indicate that, in concentrated lysozyme ethanol−water solution, following the heat-induced protein denaturation, a further reorganization of the molecular conformation takes place yielding, in long time limit, to the formation of a transparent gel. The kinetics of the gel formation and the properties of end products depend on the temperature at which the isothermal heating occurs.

## 2. EXPERIMENTAL SECTION

**2.1. Materials.** Hen egg-white lysozyme (purity ≥90%) was purchased from Sigma-Aldrich and used without further purification. Lysozyme molecule has 129 amino acid residues and a molecular weight of 14.3 kDa with an isoelectric point of 10.7 and an ellipsoidal shape characterized by semiaxes 1.9 × 2.2 × 1.1 nm.

The desired quantity of protein ($C$ = 50 and 120 mg/mL) was dissolved in ethanol−water mixture (ethanol mole ratio $X$ = 0.18) and the pH adjusted to the value of pH = 3.0. In these conditions, the protein has a positive net charge which, at room temperature, prevents protein aggregation.

**2.2. Dielectric Relaxation Measurements.** The dielectric and conductometric properties of lysozyme in ethanol−water solutions have been measured in the frequency range from 10 kHz to 2 GHz by means of frequency-domain dielectric spectroscopy, using two Precision RF impedance analyzers, Hewlett-Packard mod. 4294A (in the frequency range from 10 kHz to 110 MHz) and mod. 4291A (in the frequency range from 1 MHz to 2 GHz). The dielectric cell consists of a short section of a cylindrical coaxial cable connected to the meter by means of a precision APC-7 connector. Electrical constants of the measuring cell have been determined by a calibration procedure with three standard liquids of known conductivity and dielectric constant. In the high-frequency range of the frequency window investigated, the dielectric properties of the sample were determined from the complex reflection coefficient $\rho^*(\omega)$ by means of the relationship

$$\varepsilon^*(\omega) = \frac{A_1(\omega)\rho^*(\omega) - A_2(\omega)}{A_3(\omega) - \rho^*(\omega)} \quad (1)$$

where $A_j(\omega)$ ($j$ = 1, 2, 3) are three frequency-dependent complex constants determined by three standard measurements at each frequency point. Details of the dielectric cell and the calibration procedure have been reported elsewhere.[21−23] The dielectric measurements have been carried out in the temperature range from 20 to 60 °C, within 0.1 °C.

Within the above stated experimental procedure, the uncertainties on the permittivity $\varepsilon'(\omega)$ and the electrical conductivity $\sigma(\omega)$ are within 1.5 and 0.5% respectively, over the whole frequency range investigated.

**2.3. Dynamic Light Scattering Measurements.** Dynamic light scattering measurements were performed by means of Brookhaven equipment, using a 10 mW power He−Ne laser operating with a vertically polarized light with wavelength $\lambda$ = 633 nm and at a scattering angle of 173°. The temperature was varied in a controlled way from 20 to 60 °C, within ±0.5 °C.

In dynamic light scattering measurements, the intensity autocorrelation function

$$g^{(2)}(\tau) = \frac{\langle I(t)I(t+\tau)\rangle}{\langle I(t)I(t)\rangle} \quad (2)$$

is related to the normalized electric field correlation function $g^{(1)}(\tau)$ by the Siegert relation[24,25]

$$g^{(2)}(\tau) = 1 + \beta[g^{(1)}(\tau)]^2 \quad (3)$$

The function $g^{(1)}(\tau)$ was analyzed in terms of distribution of relaxation times

$$g^{(1)}(\tau) = \int_0^\infty A(\Gamma)\exp(-\Gamma\tau)\,d\Gamma \quad (4)$$

with $A(\Gamma)$ the function describing the distribution of decay rates, employing the Laplace inverse transformation with the aid of the program CONTIN[26,27] which employs the constrained regularization model.

Polystyrene particles (0.176 $\mu$m in size) were simply added to the fresh lysozyme solution before the beginning of the gelation process. The particles are dispersed, at a volume fraction $\Phi$ less than $\Phi$ = 0.005, in the liquid phase and thus progressively captured inside the gel network during the time evolution. Their scattering intensity was at least 2 orders of magnitude larger than the one of the pure protein solution, and consequently the measured correlation function is directly related to the movement of the probe and no contribution arises from the movement of the protein chains.

The diffusion coefficient $D$ can be calculated from the average relaxation time $\langle\tau\rangle$

$$D = \frac{1}{\langle\tau\rangle q^2} \quad (5)$$

where $q = 4\pi n/\lambda \sin\theta/2$ is the scattering wavevector, with $n$ the refractive index of the solvent, $\lambda$ the wavelength of the incident light, and $\theta$ the scattering angle.

Figure 1 shows typical correlograms obtained with dynamic light scattering for polystyrene particles (0.176 $\mu$m in size) dispersed in a lysozyme solution during the gelation process at a constant temperature, $T$ = 50 °C. At the beginning of the gelation process, we observe a single relaxation process characterized by a single-exponential decay, whereas in long time limit, we can distinguish a relaxation mode typical of the arrested state.

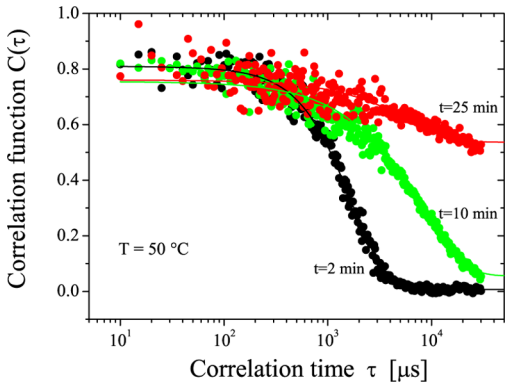


**Figure 1.** Normalized autocorrelation functions of polystyrene particles (0.176 $\mu$m in size) dispersed in a lysozyme solution during the gelation process at the temperature of $T$ = 50 °C, at different times from the beginning of the process.

**2.4. IR Measurements.** Infrared spectra were obtained by means of a Bruker FTIR spectrometer, mod. TENSOR 27. Measurements conditions and data analysis were described in detail in ref 15.

## 3. RESULTS AND DISCUSSION

**3.1. Dielectric Relaxation Results.** In ethanol–water solution, the melting temperature of lysozyme depends on the alcohol concentration. We have preliminary investigated the heat-induced denaturation process of lysozyme in ethanol–water mixture solution (mole fraction $X$ = 0.18), monitored through the changes in its dielectric relaxation spectra. In order to avoid aggregation of the unfolded protein during the melting process, in these preliminary measurements, we have confined the protein concentration to a relatively low value ($C$ = 50 mg/mL). The heat-induced denaturation process is shown in Figure 2, upper panel, where we report the dielectric parameters, i.e., the dielectric increment $\Delta\varepsilon_\beta$, the relaxation frequency $\nu_\beta$, and the dc electrical conductivity, $\sigma$, of the dielectric relaxation spectra as a function of temperature. As can be seen, protein denaturation produces a marked change in all the dielectric parameters with a denaturation temperature close to 50 °C. These findings are largely supported by IR measurements where the progressive decrease of the intensity of the 1650 cm$^{-1}$ band (Figure 2, bottom panel) is associated with the unfolding of the helix structure.[28] Both the two sets of measurements, based on different molecular probes, indicate a melting temperature close to 50 °C.

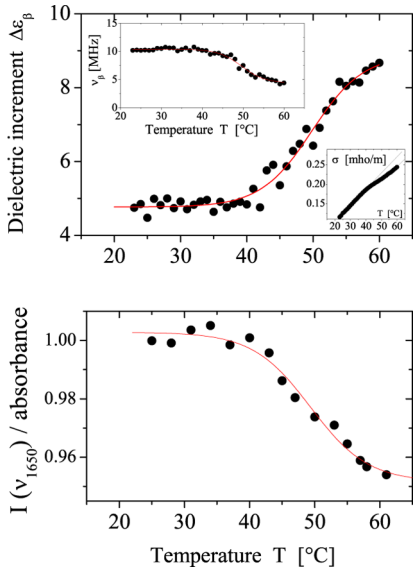


**Figure 2.** Upper panel: denaturation curve of lysozyme ($C$ = 50 mg/mL) in ethanol–water mixture (mole fraction $X$ = 0.18) as a function of temperature, as seen from the dielectric relaxation measurements. The dielectric spectra have been analyzed on the basis of the Cole–Cole relaxation function, and the dielectric parameters have been evaluated. The plot evidences the behavior of the dielectric increment $\Delta\varepsilon_\beta$, the relaxation frequency $\nu_\beta$ (inset on the left), and the dc electrical conductivity $\sigma$ (inset on the right). Bottom panel: denaturation curve of lysozyme as seen from IR measurements (absorbance at 1650 cm$^{-1}$). All the dielectric parameters and the IR absorbance indicate a denaturation temperature close to 50 °C.

*3.1.1. Protein Characterization of Native Lysozyme Solution (Before Thermal Denaturation).* As well ascertained, at frequencies higher than 1 MHz, the dielectric spectrum of lysozyme aqueous solutions consists of two main dielectric relaxation regions, termed $\beta$- and $\gamma$-dispersion, respectively, attributed to the overall rotation of the protein molecule, the former, and to the orientational polarization of the aqueous phase, the latter. In between, an accurate deconvolution of the dielectric spectra evidence a further relaxation contribution, termed $\delta$-dispersion, attributed to the polarization of the bound water at the protein surface.[29]

From the relaxation process known as the $\beta$-process, the knowledge of the dielectric increment $\Delta\varepsilon_\beta$ and the relaxation frequency $\nu_\beta$ permits the evaluation of both the protein dipole moment $\mu_{eff}$ and its hydrodynamic radius $R_H$. These parameters are linked to the dielectric parameters $\Delta\varepsilon_\beta$ and $\nu_\beta$ through the relationships[30,31]

$$\mu_{eff} = \frac{9\varepsilon_0 K_B T(2\varepsilon_s - \varepsilon_\infty)\Delta\varepsilon_\beta}{\varepsilon_s(\varepsilon_\infty + 2)N_a C} \quad (6)$$

$$R_H = \left(\frac{K_B T}{8\pi^2 \nu_\beta \eta}\right)^{1/3} \quad (7)$$

where $K_BT$ is the thermal energy, $\varepsilon_s$ and $\varepsilon_\infty$ are the low-frequency and the high-frequency limit of the permittivity $\varepsilon'(\omega)$ associated with the $\beta$-dispersion, $N_a$ is the Avogadro number, $C$ is the protein concentration, and $\eta$ is the viscosity of the aqueous medium. Figure 3 shows a typical example of the


dx.doi.org/10.1021/jp305939h | J. Phys. Chem. B 2012, 116, 10779–10785

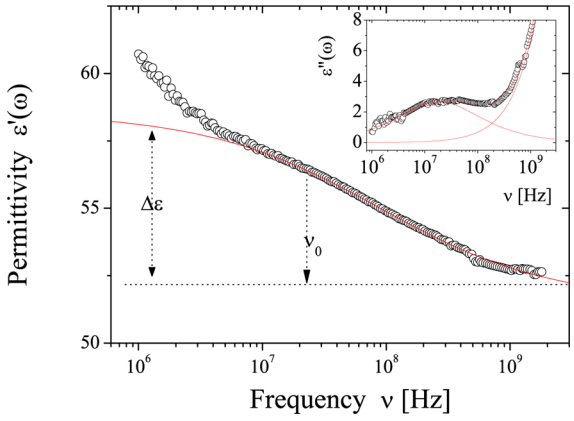


**Figure 3.** Permittivity $\varepsilon'(\omega)$ as a function of frequency of lysozyme in water−ethanol mixture (mole fraction $X = 0.18$), at the temperature of 25 °C. The protein concentration is $C = 120$ mg/mL. The inset shows the dielectric loss $\varepsilon''(\omega)$ as a function of the frequency. The full lines are the calculated values according to a Cole−Cole relaxation function. The whole relaxation process is due to the different contributions, i.e., the orientational relaxation of the protein dipole and the orientational polarization of the water molecules, in the higher frequency tail. These single contributions are shown as continuous lines.

$\beta$-dispersion of lysozyme ($C = 120$ mg/mL) in ethanol−water mixture (at a molar ratio $X = 0.18$) at the temperature of 25 °C. The analysis of the spectrum yields values of $\mu_{eff} = 125$ D and $R_H = 14$ Å, assuming a viscosity $\eta$ of ethanol−water mixture interpolated from literature data ($\eta = 2.23$ mPa s). These values compare reasonably well with the ones derived by Bonincontro et al.,[32] who investigated the influence of ethanol on the lysozyme conformation at a relatively low protein concentration ($C = 5$ mg/mL). In a previous work,[29] some of us investigated the dielectric spectra of lysozyme solution in water (pH = 5.5) at the temperature of 25 °C, up to a protein concentration of 125 mg/mL. In that case, we extended dielectric measurements up to 50 GHz, giving us the possibility to completely analyze the intermediate relaxation process as due to the superposition of the $\beta$-dispersion (motion of the protein as a whole and relaxation of the protein dipole) and the $\delta$-dispersion (hydration water in the interfacial region surrounding the protein). We observed, at the temperature of 25 °C, a relaxation frequency of the $\beta$-dispersion of about $\nu_\beta = 11$ MHz, corresponding to a hydrodynamic radius of $R_H = 17.9$ Å. In the present case, the lack of high-frequency measurements prevents the possibility to deconvolute the intermediate dispersion into the $\beta$- and $\delta$-contributions, resulting in a total relaxation frequency a little bit higher than the one coupled to the $\beta$-relaxation solely. However, these aspects lie outside the aim of the present paper, which is mainly focused on the temperature-induced gelation behavior.

*3.1.2. Protein Characterization of Heat-Denatured Protein Solution.* In the thermal denaturation, the globular structure of the native protein is transformed into a unfolded state which exposes hydrophobic groups to the aqueous solvent. Compared with native lysozyme solutions, both the dielectric increment $\Delta\varepsilon_\beta$ and the relaxation frequency $\nu_\beta$ markedly changes. In the sample of relatively low protein concentration ($C = 50$ mg/mL), i.e., in the absence of any aggregation process as revealed by IR measurements, the thermal denaturation is completed at the temperature of 60 °C (see Figure 2, bottom panel). In these conditions, with respect to the protein in the native conformation ($T = 25$ °C), we observe, accompanied by an increase of the dielectric increment, a decrease of the relaxation frequency of about 50%, passing from about 10 MHz at 25 °C to about 5 MHz at 60 °C. This change reflects an increase of the hydrodynamic radius, on the basis of eq 7 of about 25%, in qualitative agreement with results from dynamic light scattering measurements[33] and in agreement with the value of $R_H$ calculated by SAXS measurements[34] performed on lysozyme unfolded by urea (pH = 2.9), where $R_H$ changed from 15.3 to 21.8 Å for the native and unfolded protein, respectively.

Heat-denatured lysozyme presents a dielectric increment larger than the one of the native protein. This finding can be justified by the rise of a further relaxation mechanism, due to a micro-Brownian movement of the peptide chains. This contribution was proposed by Mashimo and co-workers,[35−37] who attributed the relaxation of poly($\alpha$-amino acid) aqueous solution to peptide chain motion, since the dielectric increment depended on the side-group motion, reflecting micro-Brownian motion of the polymer chains. Heating induces the exposure of hydrophobic groups, and the process could enhance the mobility of peptide chains and consequently the dielectric relaxation strength due to micro-Brownian motion increases.

*3.1.3. Protein Characterization in Isothermal Heating in the Melting Range.* We preliminary observe that in the high concentration sample ($C = 120$ mg/mL, see inset of Figure 7) the IR measurements as a function of temperature (values collected for each temperature within the first 2 min) agree quite well with those concerning the sample at low protein concentration ($C = 50$ mg/mL). This agreement suggests that, in both samples, the same melting process dominates in the first period of time, independently of protein concentration, and only further, in the sample at higher concentration, the aggregation (and gelation) occurs.

In the temperature interval where IR measurements (Figure 2, bottom panel) evidenced conformational changes in heat-denatured protein, we have measured as a function of time the dielectric spectra of lysozyme solutions ($C = 120$ mg/mL) at the temperatures of 40, 45, 50, and 60 °C. The samples, initially at room temperature, are rapidly brought to the temperature of the experiment and, from now on, the dielectric measurements started.

We have followed the time evolution of the dielectric spectra up to about 60 min and the characteristic parameters, i.e., the dielectric increment $\Delta\varepsilon_\beta$, the relaxation function $\nu_\beta$, and the dc electrical conductivity $\sigma$ as a function of time are shown in Figures 4−6.

At the temperature of 40 °C, before the beginning of the denaturation process, as indicated by the changes in the intensity of the 1650 $cm^{-1}$ (see inset Figure 7), both the dielectric increment $\Delta\varepsilon_\beta$ and the relaxation frequency $\nu_\beta$ do not vary upon time, indicating that the protein maintains its native conformation. In these conditions, the dielectric response is completely accounted for by the tumbling motion of the lysozyme molecule within the classical hydrodynamic model (eqs 6 and 7).

At higher temperatures, with the progressive unfolding of the protein, characterized by an increase of the dielectric increment from the value of globular conformation, there is a continuous evolution of the dielectric parameters as a function of time which monitors the occurring of a further structural rearrangement. In the long time limit, a gelation occurs and the system reaches an identical stationary state, proved by the same value of the dielectric increment at the three temperatures of 45, 50, and 60 °C (this tendency is a little bit less evident in the


dx.doi.org/10.1021/jp305939h | J. Phys. Chem. B 2012, 116, 10779−10785

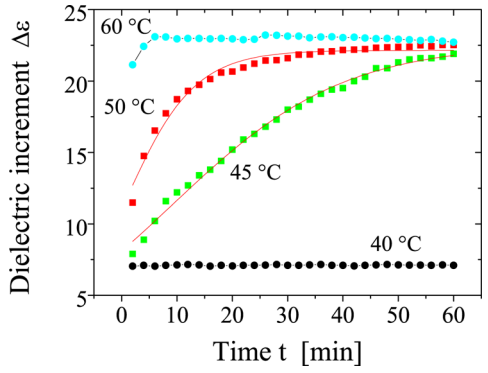


**Figure 4.** Dielectric increment $\Delta\varepsilon$ of lysozyme ($C$ = 120 mg/mL) in ethanol–water solution (mole fraction $X$ = 0.18) as a function of time at four temperatures ($T$ = 40, 45, 50, and 60 °C) in the temperature range where denaturation occurs.

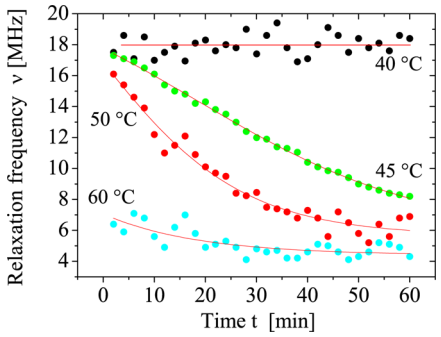


**Figure 5.** Relaxation frequency $\nu$ of lysozyme ($C$ = 120 mg/mL) in ethanol–water solution (mole fraction $X$ = 0.18) as a function of time at different temperatures above the denaturation temperature.

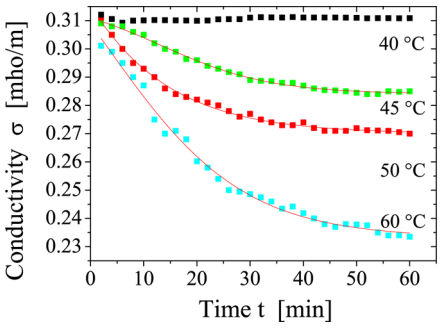


**Figure 6.** The dc electrical conductivity $\sigma$ of lysozyme ($C$ = 120 mg/mL) in ethanol–water solution (mole fraction $X$ = 0.18) as a function of time at different temperatures above the denaturation temperature.

behavior of the relaxation frequency $\nu_\beta$). Conversely, the time evolution is different, the higher temperature process being faster than the lower one.

At the highest temperature investigated ($T$ = 60 °C), almost the totality of the protein molecules are in the unfolded conformation (see Figure 2, bottom panel, and the inset of Figure 7) and the gelation occurs on a time scale longer than unfolding process (see below). Both the dielectric increment $\Delta\varepsilon_\beta$ and the relaxation frequency $\nu_\beta$ are, to a first approximation, rather independent of time, suggesting that the gelation does not modify markedly the mechanism of the dielectric relaxation.

At the intermediate temperatures (45 and 50 °C), we observe that, after the initial changes of both $\Delta\varepsilon_\beta$ and $\nu_\beta$, due to

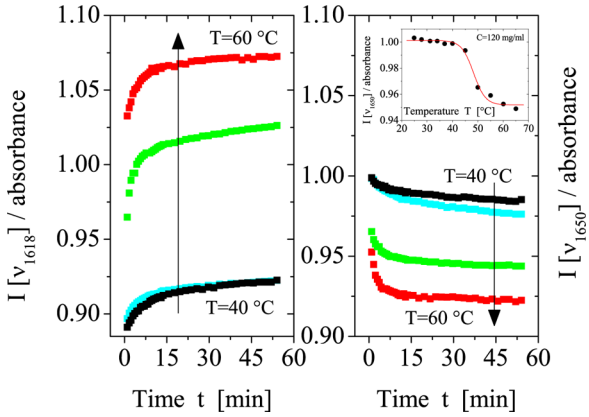


**Figure 7.** Left panel: increase of the IR intensity at 1618 $cm^{-1}$ measured on spectra of lysozyme ($C$ = 120 mg/mL) in ethanol–water mixture (mole fraction $X$ = 0.18) at different temperature from 40 to 60 °C, as a function of time. Right panel: decrease of the IR intensity at 1650 $cm^{-1}$ at different temperature from 40 to 60 °C, as a function of time. The inset shows the melting process as a function of temperature from 20 to 65 °C. These data show a very good agreement with the ones concerning the sample at lower concentration ($C$ = 50 mg/mL, see bottom panel of Figure 2).

the partial unfolding of the protein molecules, the further temporal changes indicate that the gelation process is accompanied by a further change in the protein conformation. Although size and shape are only slightly perturbed by heat denaturation,[38] the process favors internal hydrophobic groups to flip toward the outside of the protein. These conformational changes cause a further aggregation process in order to reduce the exposure of hydrophobic groups to the aqueous solvent.

The same qualitative scenario can be suggested by FTIR spectroscopy measurements. For the above-stated selected temperatures, the time evolution of the IR intensities at 1618 and 1650 $cm^{-1}$ is shown in Figure 7. As can be seen, the absorbance at 1650 $cm^{-1}$, after the initial decrease due to the melting process (see Figure 2), continues to decrease to lower values (different for each of the temperatures investigated), suggesting, in agreement with dielectric results, that the isothermal heating induces a further conformational change which evolves in a gel formation. The absorbance at 1618 $cm^{-1}$, which is practically negligible at temperatures lower than 40 °C (absence of aggregated species), increases as a function of time, reaching a steady-state value, in long time limit. At $T$ = 50 and 60 °C, the initial intensity of 1618 $cm^{-1}$ absorption suggests that a fast aggregation process occurs within the first 60 s of measurement. Also in this case, the different value reached at different temperatures may indicate that the temperature of the isothermal heating influences the characteristics of the gel formation, particularly the aggregation kinetics and the number of junctions of the active sites of the protein increases with the increase of temperature.

However, the two effects (presence of a fraction of unfolded proteins and protein aggregation), occurring concomitantly, cannot be easily separated, even if we are induced to consider that the presence of a fraction of unfolded proteins is the prerequisite for the aggregation before and the gelation after to occur.

Through heat-denaturing, hydrophobic regions, packed inside the native lysozyme, are now exposed to the surface producing intermolecular hydrophobic interactions of denatured lysozyme yielding aggregation and finally gelation. Our


dx.doi.org/10.1021/jp305939h | J. Phys. Chem. B 2012, 116, 10779–10785

experimental results suggest that this aggregation is characterized by the formation of $\beta$-sheet intermolecular structures giving a transparent gel. In long time limit, the protein solution reaches a stationary state.

Let us turn now to the other important parameter that can be derived from dielectric measurements. The electrical conductivity $\sigma$ of lysozyme solutions at temperature above the denaturation temperature is shown in Figure 6. These results can be qualitatively explained by the restriction of the mobility of ions following the change of the viscosity of the solvent phase. According to the Walden's rule

$$\frac{\sigma\eta}{C_s} = \text{const} \tag{8}$$

which relates the electrical conductivity $\sigma$, the viscosity $\eta$, and the ionic concentration $C_s$, the electrical conductivity, as the viscosity of the medium increases, is expected to decrease, provided that the ion concentration $C_s$ is constant. It is worth to note that, in long time limit, conductivity assumes values which decrease with the increase of temperature, opposite to what happens in unconfined media, suggesting once more that the reduction of mobility because of the viscosity increase becomes a dominant factor. Moreover, as can be seen, in long time limit, the electrical conductivity reaches values different for the isothermal heating at the different temperatures investigated. This finding is a further print of the fact that gels with different numbers of junctions in the different reacted sites are forming, reflecting in a different viscosity.

**3.2. Dynamic Light Scattering Results.** The translational diffusion characteristics of monodisperse polystyrene latex particles (0.176 $\mu$m in size), deliberately added to the lysozyme solutions, have been measured during the process of gel formation above the denaturation temperature. Since the scattered light intensity of latex particles at the melting temperatures is well above the background of the protein solution, their diffusion coefficient can be considered as a probe which indirectly responds to the topological changes occurring in the solution during the gelation. In this way, we have monitored the gel formation through the time evolution of the apparent diffusion coefficient $D$ of our probe. The presence of a gel network creates a difficulty for translational diffusion of polystyrene particles entrapped in the aqueous phase that is itself retained in the solid network. The progressive decrease of the apparent diffusion coefficient is attributed to the growing level of geometric constrains during the gel formation which impede the particle translational motion, and consequently, thanks to the temporal decrease of the apparent diffusion coefficient $D$, we are able to monitor the concomitant buildup of the gel phase, as the gelation proceeds.

As can be seen in Figure 1, at the beginning of the time interval, the correlation function is well-represented by a single relaxation time, and the data fit fairly well with a single process characterized by a single diffusion coefficient whose value matches with the one expected for a 0.176 $\mu$m particle in water at the temperature of the experiment.

As time goes on, correlation functions shift to the right, deviating from a single-exponential decay and indicating a progressive decrease in the diffusion coefficient. This suggests that a structural change takes place in the protein solution.

Typical results are shown in Figure 8, where we report the diffusion coefficient $D$ of polystyrene latex particles embedded into the protein solution, at two temperatures above the denaturation temperature.

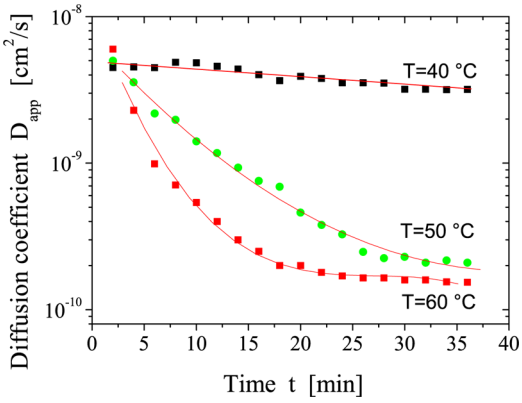


**Figure 8.** Apparent diffusion coefficient $D$ of polystyrene particles (0.176 $\mu$m in size) dispersed in a lysozyme solution during the gelation process, at different times from the beginning, at different temperatures in the melting range.

Moreover, from the diffusion coefficient and the known effective hydrodynamic radius of the particle, with the aid of the Stokes–Einstein equation, it is possible to obtain the microviscosity $\eta$ of the solution near the probe environment. Figure 9 shows the apparent microviscosity of the protein

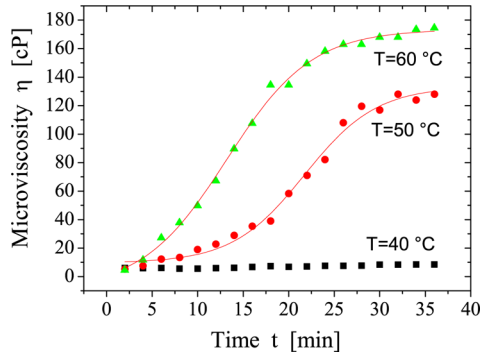


**Figure 9.** Microviscosity $\eta$ of the lysozyme solution as calculated from the diffusion coefficient $D$ on the basis of the effective hydrodynamic radius of the polystyrene latex particles (0.176 $\mu$m in size), at different temperatures at the melting temperatures.

solution calculated from the diffusion coefficient $D$ and the hydrodynamic radius of the polystyrene particles. The rapid increase of the microviscosity at temperatures above the denaturation temperature indicates the progressive gelling of the system as time goes on. It is worth noting that both the diffusion coefficient $D$ and the microviscosity $\eta$, in long time limit, reach a limiting value that depends on the temperature. These results give a picture of the gel consisting of rather large aqueous compartments, where particle probes are trapped, enclosed by dense walls, which probes are unable to penetrate. As the temperature increases above the denaturation temperature, the number of cross-links increases and the compartment size becomes smaller.

## 4. CONCLUSIONS

This study was intended to provide additional insights into the heat-induced denaturation and concomitant gelation processes of lysozyme by analyzing the dielectric parameters of the protein solution in the frequency range from 1 MHz to 2 GHz, where the dielectric response is indicative of the tertiary


dx.doi.org/10.1021/jp305939h | J. Phys. Chem. B 2012, 116, 10779–10785

structure of the protein. We have observed that, by virtue of the heat-induced melting, once a fraction of unfolded molecules is produced, when protein concentration is high enough, an aggregation process occurs which ends, in long time limit, when the whole system gels. This picture is also sustained by FTIR spectroscopic measurements of the amide I band, where the absorbance at 1618 and 1650 $cm^{-1}$ clearly evidences both the melting of the protein and its aggregation.

It is worth noting that a fast formation of ordered clusters is observed at the beginning of the aggregation process for a concentrated lysozyme sample. This initial formation does not perturb the unfolding process, and the absorption intensity at 1650 $cm^{-1}$ has the same temperature behavior as the one shown by the sample at concentration of 50 mg/mL. Moreover, a different amount of intermolecular contacts is established at 50 and 60 °C; this difference is observed also at long time limit as well as other techniques evidence.

The formation of a transparent gel, in long time limit, has been monitored by means of dynamic light scattering measurements, taking advantage of a probe deliberately added to the protein solution. Its diffusion coefficient is an indirect measure of the microviscosity in the close environment and hence is an index for the gel formation. Our measurements, all together, indicate that in high concentration systems the heat-induced melting is followed by a further process, where unfolded proteins first aggregate and then form, in long time limit, a transparent gel. The gelation kinetics differs accordingly to the temperature at which the isothermal heating occurs. In long time limit, we obtain more or less the same values of dielectric parameters, both the dielectric increment and the relaxation frequency, at 45, 50, and 60 °C. Moreover, these values are those measured for the unfolded state of the low concentration lysozyme solution, indicating that an unfolded tertiary structure is characteristic of the gel. On the contrary, microviscosity, $\alpha$-helix fraction, and electrical conductivity measurements indicate that a different thermal treatment can define different properties of the gel phase for the same ternary system. These findings could suggest the possibility of regulating micro- and macroscopic properties of the system by selecting appropriate heating temperatures.

## AUTHOR INFORMATION

### Corresponding Author

*Fax +39 06 4463158; e-mail cesare.cametti@roma1.infn.it.

### Notes

The authors declare no competing financial interest.

## REFERENCES

(1) da Silva, M. A.; Areas, E. P. G. *J. Colloid Interface Sci.* **2005**, *289*, 394−401.
(2) Gosal, W. S.; Ross-Murphy, S. B. *Curr. Opin. Colloid Interface Sci.* **2000**, *5*, 188−194.
(3) Yan, H.; Frielinghaus, H.; Nykanen, A.; Roukolainen, J.; Saiani, A.; Miller, A. F. *Soft Matter* **2008**, *4*, 1313−1325.
(4) Tani, F.; Murata, M.; Higasal, T.; Goto, M.; Kitabatake, N.; Doi, E. *J. Agric. Food Chem.* **1995**, *43*, 2325−2334.
(5) Takeuchi, Y.; Uyama, H.; Tomoshige, N.; Watanabe, E.; Tachibana, Y.; Kobayasi, S. *J. Polym. Sci., Part A: Polym. Chem.* **2006**, *44*, 671−675.
(6) Jonker, A. M.; Lowik, D. W. P. M.; van Vest, J. C. M. *Chem. Mater.* **2012**, *24*, 759−773.
(7) Nicolai, T.; Durand, D. *Curr. Opin. Colloid Interface Sci.* **2007**, *12*, 23−28.
(8) Sassi, P.; Perticaroli, S.; Comez, L.; Lupi, L.; Paolantoni, M.; D, F.; Morresi, A. *J. Raman Spectrosc.* **2012**, *43*, 273−279.
(9) Castelletto, V.; Areas, E. P. G.; Areas, J. A. G.; Craievich, A. F. *J. Chem. Phys.* **1998**, *109*, 6133−6139.
(10) da Silva, M. A.; Areas, E. P. G. *Biophys. Chem.* **2002**, *99*, 129−141.
(11) da Silva, M. A.; Iri, R.; Areas, E. P. G. *Biophys. Chem.* **2002**, *99*, 169−179.
(12) da Silva, M. A.; Areas, E. P. G. *J. Colloid Interface Sci.* **2005**, *289*, 394−401.
(13) da Silva, M. A.; Farhat, I. A.; Areas, E. P. G. *Biopolymers* **2006**, *83*, 443−454.
(14) Areas, E. P. G.; Areas, J. A. G.; Hamburger, J.; Peticolas, W. L.; San-tos, P. S. *J. Colloid Interface Sci.* **1996**, *180*, 578−589.
(15) da Silva, M. A.; Areas, E. P. G. *Biophys. Chem.* **2002**, *99*, 129−141.
(16) da Silva, M. A.; Itri, R.; Areas, E. P. G. *Biophys. Chem.* **2002**, *289*, 169−179.
(17) Tanaka, S.; Oda, Y.; Ataka, M.; Onuma, K.; Fujiwara, S.; Yonezawa, Y. *Biopolymers* **2001**, *59*, 370−381.
(18) Sassi, P.; Giugliarelli, A.; Paolantoni, M.; Morresi, A.; Onori, G. *Biophys. Chem.* **2011**, *158*, 46−53.
(19) Furusawa, H.; Ito, K.; Hayakawa, R. *Phys. Rev. E* **1997**, *55*, 7283−7287.
(20) Mitsumata, T.; Gong, J. P.; Ikeda, K.; Osada, Y. *J. Phys. Chem. B* **1998**, *102*, 5264−5251.
(21) Bordi, F.; Cametti, C.; Colby, R. H. *J. Phys.: Condens. Matter* **2004**, *R1423*, R1463.
(22) Bordi, F.; Cametti, C.; Motta, A.; Paradossi, G. *J. Phys. Chem. B* **1999**, *103*, 5092−5099.
(23) Bao, J.-Z.; Davis, C. C.; Swicord, M. L. *Biophys. J.* **1994**, *66*, 2173−2180.
(24) Berne, B. J.; Pecora, R. *Dynamic Light Scattering*; Dover Pub. Inc.: New York, 2000.
(25) Schimitz, K. S. *An Introduction to Dynamic Light Scattering by Macromolecules*; Academic Press: San Diego, CA, 1990.
(26) Provencher, S. *Comput. Phys. Commun.* **1982**, *27*, 213−227.
(27) Provencher, S. *Comput. Phys. Commun.* **1982**, *27*, 229−242.
(28) Sassi, P.; Onori, G.; Giugliarelli, A.; Paolantoni, M.; Cinelli, S.; Morresi, A. *J. Mol. Liq.* **2011**, *159*, 112−121.
(29) Cametti, C.; Marchetti, S.; Gambi, C. M. C.; Onori, G. *J. Phys. Chem. B* **2011**, *115*, 7144−7153.
(30) Takashima, S. *Electrical Properties of Biopolymers and Membranes*; Adam Hilger: Bristol, 1989.
(31) Grant, E.; Sheppard, R.; South, G. *Dielectric Behaviour of Biological Molecules in Solution*; Clarendon Press: Oxford, UK, 1978.
(32) Bonincontro, A.; De Francesco, A.; Matzeu, M.; Onori, G.; Santucci, A. *Colloids Surf., A* **1997**, *10*, 105−111.
(33) Esposito, A.; Comez, L.; Cinelli, S.; Scarponi, F.; Onori, G. *J. Phys. Chem. B* **2009**, *113*, 16420−16424.
(34) Chen, L.; Hodgson, K. O.; Doniach, S. *J. Mol. Biol.* **1996**, *261*, 658−671.
(35) Hayashi, Y.; Miura, N.; Shinyashiki, N.; Yagihara, S.; Mashimo, S. *Biopolymers* **2000**, *54*, 388−397.
(36) Lu, Y.; Fujii, M.; Kanai, H. *Int. J. Food Sci. Technol.* **1998**, *33*, 393−399.
(37) Sun, Y.; Ishida, T.; Hayakawa, S. *J. Agric. Food Chem.* **2004**, *52*, 2351−2357.
(38) Matsumoto, T.; Inore, H. *J. Chem. Soc., Faraday Trans.* **1991**, *87*, 3385−3388.